20056118

116 The Flow and Mixing Characteristics of the Fresh Air and EGR Gas for Various Mixer Configurations at Intake Manifold System

(1) *(2) (3) (3)

Jin Nam KIM, Ho Young KIM, Won Geun LEE, Woo Tae KIM

(1) *(2) (3)

Department of Mechanical Engineering, Korea University, Hyundai Motor Co., Ltd

Anam-dong Sungbuk-ku, Seoul 136-701, Korea

EGR is a primary emission control technique for the suppression of NOx. However, combustion instability is occurred occasionally due to mal-distribution of fresh air and EGR gas at each cylinder. To improve EGR distribution characteristics, numerical simulations are performed to obtain the flow and mixing characteristics and the EGR gas distribution at each cylinder for various EGR gas mixer configurations in a 4-cylinder engine. The results show that slit type mixer has better EGR gas distribution compare with other types of mixer including the basic mixer.

***Keyword*: Research & Development, Pollution / EGR, Mixer Configuration, Distribution, Mixing, Flow field**

1. INTODUCTION

Development of advanced engine control systems for the modern 4-stroke gasoline engine is being driven by demand for higher fuel economy and increasingly stringent exhaust emissions standards. Additionally, emissions compliance must be maintained for increasing service duration while On-Board-Diagnostics (OBDII) requirements are satisfied. However, it is difficult to improve the DeNOx technology due to combustion stability and fuel economy.

Exhaust Gas Recirculation (EGR) is an established primary emission control technique for the effective suppression of NOx emissions in reciprocating internal combustion engine. Gasoline engines, depending on their operating condition, have the capability to recirculate up to 20 percent of the exhaust gases without affecting combustion stability. Gasoline Direct Injection (GDI) technology offers potential for more substantial EGR rates to be tolerated [(1)]. However, combustion instability is occurred occasionally due to mal-distribution of fresh air and EGR gas at each cylinder. Nevertheless, the study about both EGR distribution and flow characteristics for various EGR gas supplying system at intake manifold system is insufficient [(2-4)].

In this study, numerical simulations are performed to obtain the EGR gas distribution at each cylinder for various EGR gas mixer configurations in a 4-cylinder engine. The new mixer configurations are suggested in order to improve the mixing characteristics of the basic mixer which is using presently.

2. MATHEMATICAL MODEL

2.1 EGR mixers

Figure 1 shows schematics of the new mixer and the basic mixer. For basic mixer which is installed after the throttle body, the exhaust gas is directly supplied to the fresh air inlet pipe through the breather pipe. To improve the mixing characteristics between fresh air and exhaust gas, however, the new mixer has an additional supply line shaped of ring, which supplies exhaust gas in three directions to the fresh air inlet pipe through three mixer holes.

As shown Fig. 1, the two mixer holes located to the breather pipe(the mixer hole number 1 and 2) have a symmetrical arrangement from horizontal, where Θ is called mixer hole angle. This angle is changed from 30^o to 90^o by 10^o in the numer-

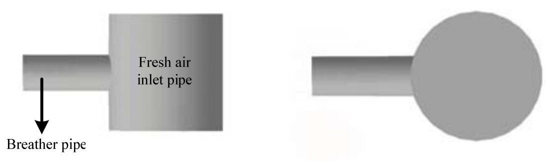

(a) Basic mixer

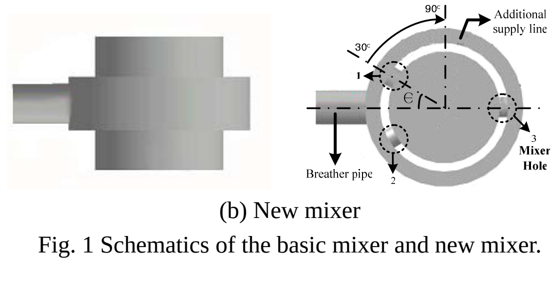

(b) New mixer

Fig. 1 Schematics of the basic mixer and new mixer.

ical simulation. The position of the last mixer hole (the mixer hole number 3) is the opposite direction of the breather pipe and fixed. Each area of mixer holes is same and the total area of them is identical compared with that of breather pipe. The breather pipe is situated just downstream of the valve (45 mm from the pivot), in-line with the pivot shaft. The thickness of the additional supply line is 3 mm with 30 mm of width. The mixer hole is 2 mm in length.

2.2 Governing equation

The conservation equations for mass, momentum and scalar variables for turbulent flow can be described as equation (1), with the variables given in Table 1.

$$\frac{\partial}{\partial t}(\rho\varphi)+\frac{\partial}{\partial x_j}\left(\rho u_j\varphi\right)=\frac{\partial}{\partial x_j}\left(\Gamma_\varphi\frac{\partial\varphi}{\partial x_j}\right)+S_\varphi \qquad (1)$$

The compressible flow modeling is essential due to the high-speed local flows in the throttle body. These effects are considered through the equation of state shown in equation (2),

$$p=\rho RT \qquad (2)$$

In the present study, it is assumed that exhaust gas consists of N_2, H_2O, CO_2, CO, H_2 and O_2. With experimental data and equation (3), the exhaust gas is assumed as a mono-component gas. Temperatures of each exhaust gas are assumed about 668 K. Properties of mono-component exhaust gas are as shown in Table 2.

$$C_nH_m+(n+m/4)\lambda(O_2+3.714N_2+0.048Ar)\Rightarrow\sum\left(b_i\bullet S_i\right) \qquad (3)$$

3. NUMERICAL METHODS

3.1 Mesh generation

The intake manifold system and throttle body used in the present study are components of 4 cylinder 1500cc gasoline engine. Meshing on the full geometry utilizes CAD models of intake manifold system and throttle body that is manually created from basic geometric data.

Computationally, the domain has been modeled by two parts. Firstly, the throttle body has a small thin crescent which must be modeled well in order to obtain good results, thus tetrahedral mesh is generated in this region. Secondly, a hexahedral mesh is generated for the surge-tank, runners and fresh air inlet pipe. The calculation domain has about 380,000 cells. Fig. 2 shows the tetrahedral mesh for the throttle body and the generated mesh of EGR supply system.

Table 1 Generalized equation

Equation	φ	Γ_φ	S_φ
Continuity	1	0	0
Momentum	u_i	μ_e	$-\frac{\partial p}{\partial x_i}+\frac{\partial}{\partial x_j}\left(\mu_e\frac{\partial v_j}{\partial x_i}\right)$
Turbulent kinetic energy	k	$\frac{\mu_e}{\sigma_k}$	$G_k-\rho\varepsilon$
TKE dissipation rate	ε	$\frac{\mu_e}{\sigma_\varepsilon}$	$\frac{\varepsilon}{k}\left(c_1G_k-c_2\rho\varepsilon\right)$
Species	Y_s	$\frac{\mu_e}{\sigma_Y}$	0
Energy	h	$\frac{\mu_e}{\sigma_h}$	0

Where, $G_k=\mu_t\left(\partial u_i/\partial x_j+\partial u_j/\partial x_i\right)\partial u_i/\partial x_j$; $\mu_e=\mu+\mu_t$; $\mu_t=\rho c_\mu k^2/\varepsilon$:

3.2 Numerical procedure

Time-dependent solutions are initiated using steady-state enhanced viscosity results that have been allowed to reach their maximum level of convergence. The next step uses these results as the initial flow field for turbulent transient analysis. However, because of the instability of the numerical calculation, calculations are conducted for several cycles. Finally, the results of the last cycle are used to examine the mixing characteristics and EGR mal-distribution at each cylinder.

Determination of the appropriate time step for calculations is based on the average flow speed in the domain, and the non-dimensional quantity, the Courant number. In the present study, the size of time step is 1^o CA for 2000 rpm of operating condition. The fully implicit scheme is utilized for time marching calculation.

Turbulence modeling has made use of the standard k-ε model for high Reynolds number flows. PISO algorithm is applied to solve the flow fields with upwind differencing schemes used to calculate pressure and velocity values.

Table 2 Properties of exhaust gas

Molecular weight	29.5 kg/kmol
Density	0.4557 kg/m^3
Specific heat	1.319E+0.3 J/kgK
Viscosity	2.8447E-05 kg/ms
Conductivity	0.0366 W/ms

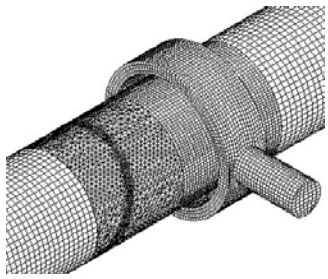

(a) Tetrahedral mesh for the throttle body

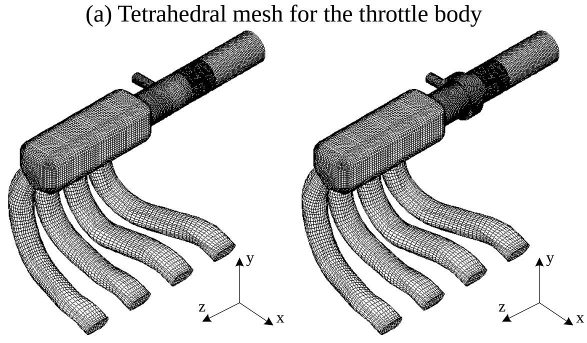

(b) Basic mixer (c) New mixer

Fig. 2 Generated mesh of EGR supply system

Table 3 Inlet boundary conditions

	Boundary type	Turb. Intensity(m^2/s^2)	Length scale(m)
Air inlet	Pressure(1bar)	$(\text{Inlet velocity}*0.1)^2$	Inlet Dia.× *0.1
EGR inlet	Velocity (mass flow)	$(\text{Inlet velocity}*0.1)^2$	Inlet Dia.× *0.1

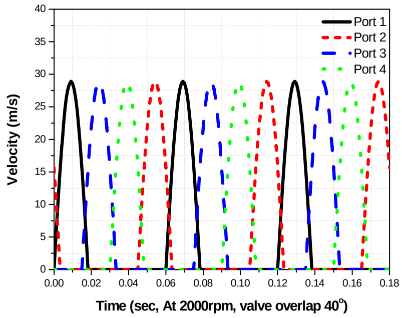

Fig. 3 Velocity profile of outlet boundary condition

3.3 Boundary condition

The inlet pressure boundary condition of fresh air is fixed at standard atmospheric pressure (1×10^5 Pa). Sanborn[5] gives a value of 5% intensity for high Reynolds number flows through a circular pipe. This value is used in conjunction with a length scale of 2.45×10^{-3} m (based on 7 % of the inlet radius) to obtain initial results. In reality, the turbulence intensity is higher, thus, a squared value of 10 % intensity for inlet velocity and a value of 10 % length scale of the inlet radius are used[6]. Also, the inlet velocity boundary condition of EGR gas is fixed at EGR rate 11 % of operating condition 2,000 rpm, bmep 2 bar. Each inlet boundary condition is indicated in Table 3. Together with these, a no-slip wall boundary condition has been applied to all other surfaces.

Conceptually, in a single intake pipe of infinite length, the pressure perturbation on the upstream of the throttle valve is only dependent on the piston and valve motion. Moreover, during the intake stroke, the piston produces an instantaneous reduction of pressure in the cylinder, with respect to the pressure level in the intake manifold. Hence, if in such conditions the instantaneous pressure evolution could be monitored[7]. The results would be similar to sinusoidal in shape. Therefore, in present study, velocity profile is assumed to the shape of sinusoidal for outlet boundary condition considering experiment-tal data as shown in Fig. 3.

4. RESULTS AND DISCUSSION

Numerical simulations are carried out for the various mixer geometries using the commercial code, STAR-CD.

4.1 Validation

Since the flow after the throttle body has a important role on mixing characteristics, Comparisons between numerical results and experimental results by Kim[8] are made in order to verify the simulation results.

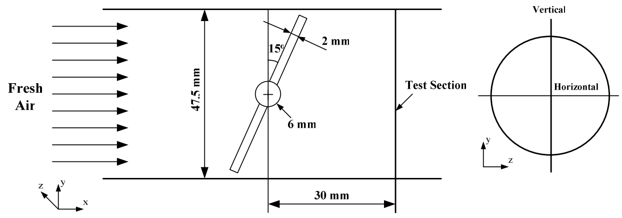

Fig. 4 Schematic of the throttle body for validation

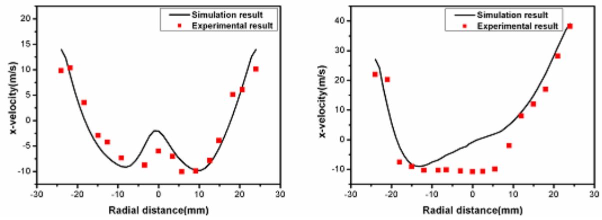

(a) Horizontal (b) Vertical

Fig. 5 Comparison with experimental results by Kim[8]

Fig. 6 Pressure drop at the throttle body, viewed through a central cross section.

In the experiment, the diameter and thickness of throttle valve are 47.5 mm and 2 mm respectively. The specification of throttle valve and the test section are shown in Fig 4. Fresh air flows at mass flow rate of 28.9 kg/h with 15° of blade angle and 10 % EGR rate. The numerical results of the u-velocity along the horizontal and vertical direction after throttle body are shown in Fig. 5, which shows the good agreement between numerical and experimental results.

In present study, Comparisons of pressure drop through the throttle body and mass flow rate of fresh air from the calculation and experiments are also made for the operating condition, 2000 rpm with 40° of valve overlap. Since the inlet pressure boundary conditions are given instead of mass flow rate in the simulation, for the given operating condition, mass flow rate and pressure drop obtained by simulations are 28.9 kg/h and 55 kpa, which are well good with the experimental results. Fig. 6 shows the pressure distribution through the throttle body.

4.2 Distribution of EGR

To improve the mixing characteristics between fresh air and exhaust gas, the new mixer having three mixer holes to induce the more infiltration of EGR gas is suggested. The ideal slit type mixer which has a slit to supply EGR gas with continuously varying width from 3 mm to 7 mm is also suggested, as shown in Fig. 7.

The mass flow rates of EGR gas are calculated for each port and summarized in Table 4. For all types of mixer, the variation of the mass flow rate of EGR gas as well as fresh air is relatively large at port 1 and port 4. This means that the flow fields of EGR gas is strongly affected by the fresh air with intense momentum after throttle body.

Figure 8 represents the standard deviation and improvement of EGR distribution for various mixers compared with basic mixer. It shows that the new mixers suggested in the present study have better EGR distribution compared with basic one. Especially, the slit type mixer has the best EGR distribution and is improved 14.75 % of standard deviation from basic mixer.

As the hole angle of the new type mixers is increased from 30^o to 60^o, the distribution characteristics is gradually improved. However, the reverse tendency is appeared with increasing mixer hole angle from 60^o to 90^o. The reason is that the interactions of complex flow fields after throttle body and the location of mixer hole affects the mixing the fresh air with the EGR gas. Therefore, it is important to analysis the flow fields at the throttle body.

4.3 Flow field analysis at the throttle body

As seen in Fig. 6, the large pressure drop of fresh air occurs through throttle body. The pressure drop and small crescent shape space make a complicate flow field, with the exhaust gas being induced through the breather pipe. The blade angle of throttle body for the given operating condition is 17^o.

Figure 9 shows that the flow passing over the trailing edge at the upper part of the valve is accelerated through the small space, attached to the wall and does not flow into the center region. On the other hand, the flow passing over the leading edge at the lower part of the valve accelerates over the tip flowing to the enter region. Also, a stagnation point is appeared on the frontal surface of valve.

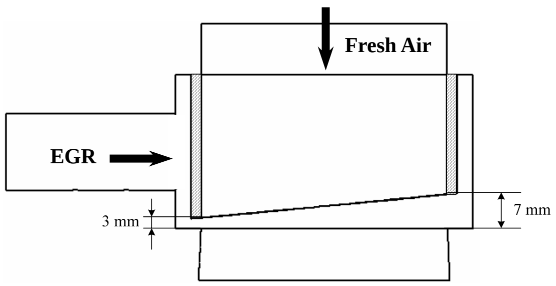

Fig. 7 Schematic of the slit type mixer

Table 4 Distribution of EGR and fresh air at each port

	Port 1(%)	Port 2(%)	Port 3(%)	Port 4(%)
Basic	30.44	23.96	24.73	20.87
Mixer 30^o	30.23	23.97	24.85	21.14
Mixer 40^o	30.15	23.67	24.89	21.23
Mixer 50^o	30.12	23.44	24.93	21.52
Mixer 60^o	29.77	23.25	25.15	21.83
Mixer 70^o	29.63	23.78	25.20	21.38
Mixer 80^o	29.64	24.13	25.24	20.98
Mixer 90^o	29.80	23.74	25.48	20.98
Slit	29.95	23.54	25.24	21.62
Fresh Air	26.75	24.51	24.82	23.92

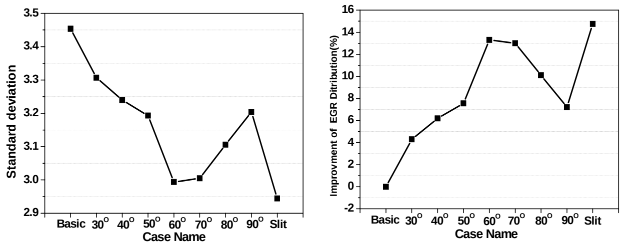

Fig. 8 Standard deviation and improvement of EGR distribution

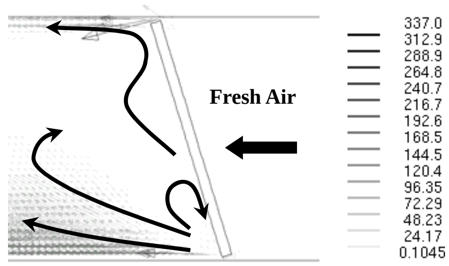

Fig. 9 Flow field around the throttle valve at central cross section

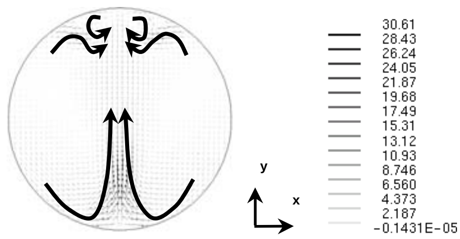

Fig. 10 Velocity vector in x-y plane after throttle body

Figure 10 represents the velocity vector in x-y plane after throttle body. It shows that the two small vortices formed by high speed trailing edge flow do not penetrate into the center region, which can be ascertained from Fig. 9.

The accelerated flows through small space at trailing and leading edge make large pressure drop between the upstream and downstream of throttle valve that leads the induction of EGR gas.

Figure 11 (a) and (b) represent the velocity vector in x-z plane and magnitude of w-velocity in x-y plane respectively. There is a reverse flow toward the throttle valve due to the low pressure. Figure 12 represents the path line of EGR gas at the full opened of intake valve for each port. It shows that the reverse flows are observed for all ports as seen in Fig. 11.

4.4 Mixing characteristics

As presented before, the high speed with intense momentum and symmetric reverse flows are occurred near the downstream of throttle valve. Thus, the locations of EGR mixer holes must be determined by considering the complicated flow after throttle body.

Contours of EGR gas mass fraction at the cross sections including hole 1 and 2 for 30^o and 90^o mixers are shown in Fig. 13. For the 30^o mixer, the driven EGR gas flows to the throttle valve by the reverse flow. However, the driven EGR gas for the 90^o mixer directly flows into the downstream due to high speed flow near the wall.

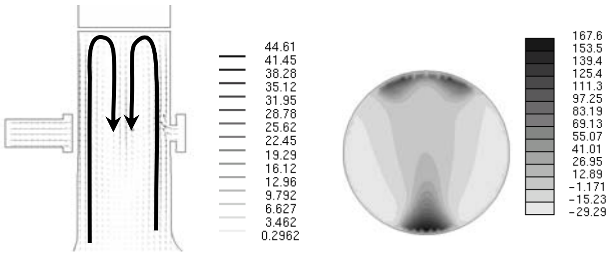

(a) x-z plane (b)magnitude of w-velocity in x-y plane

Fig. 11 Flow fields after throttle body

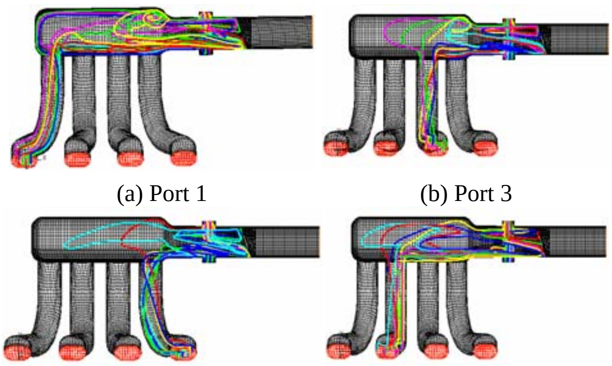

(a) Port 1 (b) Port 3

(c) Port 4 (d) Port 2

Fig. 12 Path lines of EGR gas at full opened of intake port

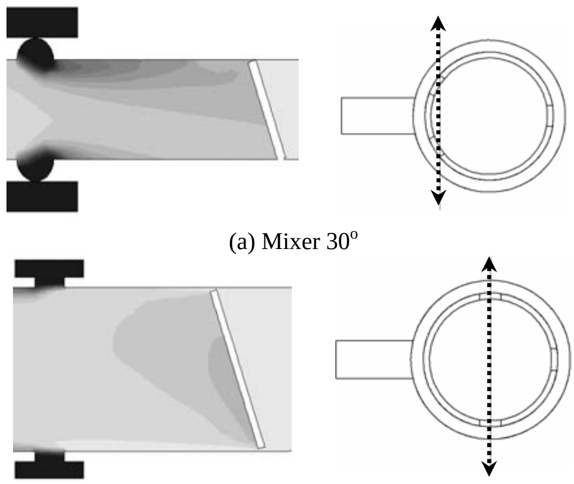

(a) Mixer 30^o

(b) Mixer 90^o

Fig. 13 Contours of EGR gas mass fraction at the cross section including hole 1 and 2

Figure 14 shows the flow at the cross section of mixers including the contour of mass fraction of EGR gas. Analyses of the results represent that the intense momentum of fresh air has greatly affected the penetration depth of EGR gas. When the mixer hole angle is from 30^o to 60^o, the mixer holes 1 and 2 are located in the region of reverse flow. As a result, the penetration depth is larger than that of other cases. Whereas, when the mixer hole angle is from 70^o to 90^o, since the mixer holes 1 and 2 are located in the region of high speed flow, the penetration depth is small.

As seen in Fig. 10, the leading edge flow spreads into the center region, whereas the trailing edge flow remains attached to the wall with intense momentum. Thus, the mixer hole of number 2 has more penetration depth with increasing mixer hole angle from 30^o to 90^o compared with that of hole 1. Moreover, the intake manifold system used present study has a large curvature between inlet pipe and port 4. Such a configuration and characteristics of the leading and trailing edge flow affect the EGR mal-distribution between port 1 and port 4.

5. CONCLUSION

The flow and mixing characteristics of the fresh air and EGR gas were predicted numerically for various mixer configurations at intake manifold system. The results represent that the new mixer has better EGR distribution characteristics compared with basic mixer. However, EGR mal distributions in the port 1 and port 4 are appeared due to intense momentum and reverse flow of fresh air after throttle body.

ACKNOWLEDGEMENT

The authors are grateful to the Hyundai Motor Company for financial support, and for granting permission to publish the findings.

REFERENCES

1. J.G. Hawley, F.J. Wallace, A. Cox, R.W. Horrocks and G.L. Bird, “Reduction of Steady State NOx levels from an Automotive Diesel Engine Using Optimised VGT/EGR Schedules,” SAE 1999-01-0835, 1999.
2. R.S.G. Baert, D.E. Beckman and A. Veen, “Efficient EGR Technology for Future HD Diesel Engine Emission Targets,” SAE 1999-01-0837, 1999.
3. H. Yokomura, S. Kohketsu and K. Mori, “EGR System in a Turbocharged and Intercooled HD Diesel Engine,” Proceedings of JSAE 20015459, Oct, 2001.
4. Ian J. Berry, Mike F.J. Brunt, “Improved Control of EGR During Speed/Load Transients,” SAE 960068, 1996.
5. V. A. Sanborn, “Application of the Hot-Wire Resistive-Temperature Transducer to the Measurement of Transient Flow Quantities,” Symposium on Measurement in Unsteady Flow, ASME Hydraulic Division Conference, Worcester Mass, pp. 54-60, 1962.
6. FIRE User’s Guide, Ver. 7.3
7. J. Benajes, “Predesign Model for Intake Manifolds in Internal Combustion Engine,” SAE 970055, 1997.
8. J. R. Kim, “The experimental Study on the Mixing Characteristics of the Fresh Air and EGR Gas for Mixer Configurations,” Thesis of Korea University, 2004.

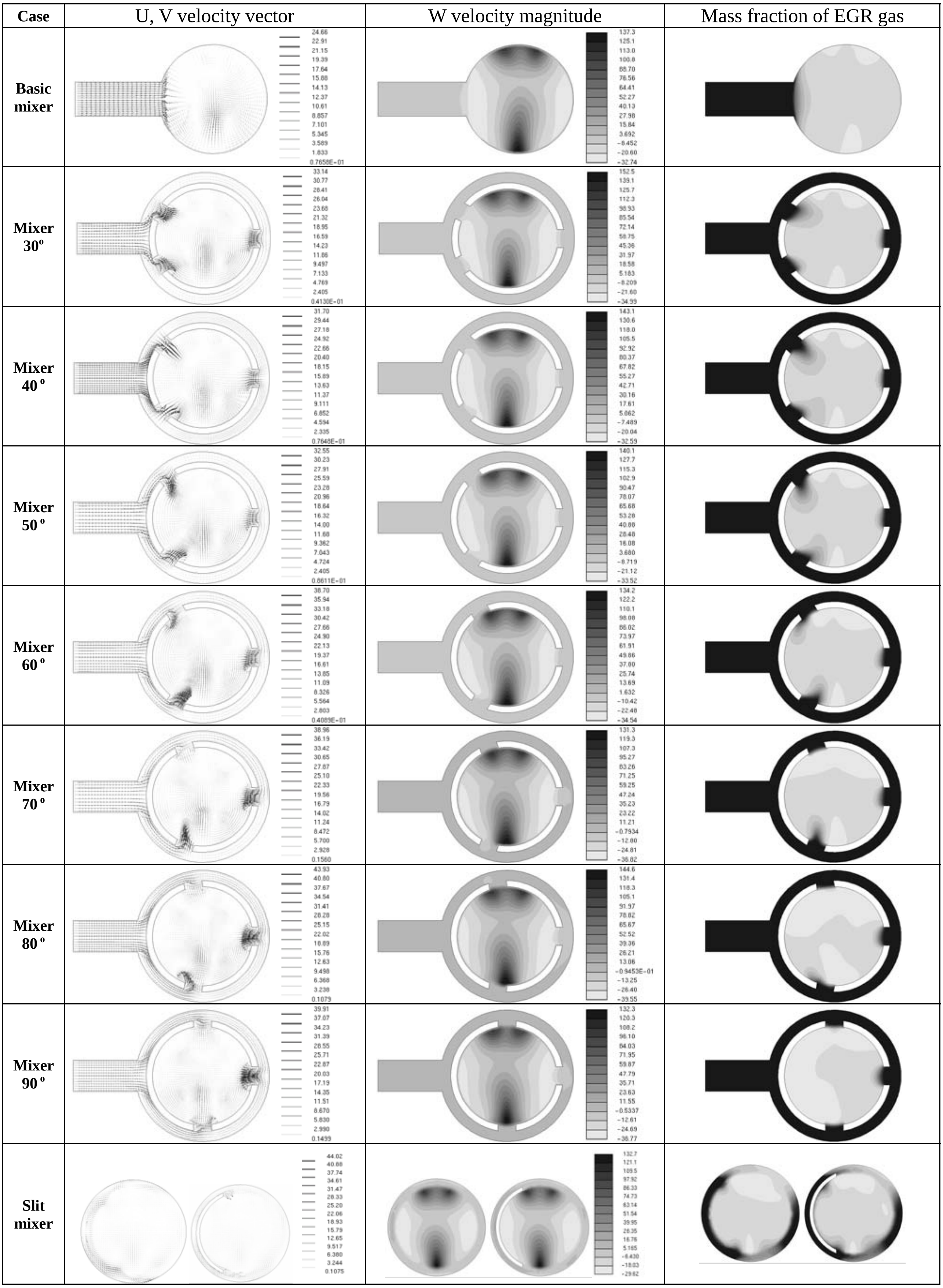

Fig. 14 Flow fields and mass fractions at the cross section of the mixers